2. A dual role for BBP/ScSF1 in nuclear pre-mRNA retention and splicing

2.1. Generation of conditional mutants of *msl5*

We first generated a collection of mutated *msl5* open reading frames (ORF) coding for BBP/ScSF1 by amplifying this DNA fragment by mutagenic PCR (Cadwell and Joyce, 1992). A library of about 13000 independent clones was created by cloning the mutagenized PCR product together with the *MSL5* wild type promoter region (259 bp) into a yeast centromeric vector (Figure 25). This should maintain expression of mutant proteins as close as possible to the wild type SF1 levels. Sequencing of eight randomly selected clones revealed a mutation rate of approximatively 1.4% at the nucleotide level (3600 bp analyzed, data not shown). Highly mutagenic conditions were favored because previous analyses failed to reveal conditional mutants in this gene. Consistently, only roughly 20% of these plasmids provided sufficient SF1 function to complement a *MSL5* disruption. The viable clones (more than 400) were subcloned on YPD plates and tested for their growth at various temperatures (16, 23, 30, 37°C). Potential mutants were selected and a second round of plasmid shuffling was performed to ensure a plasmid linked phenotype (see Materials and Methods).

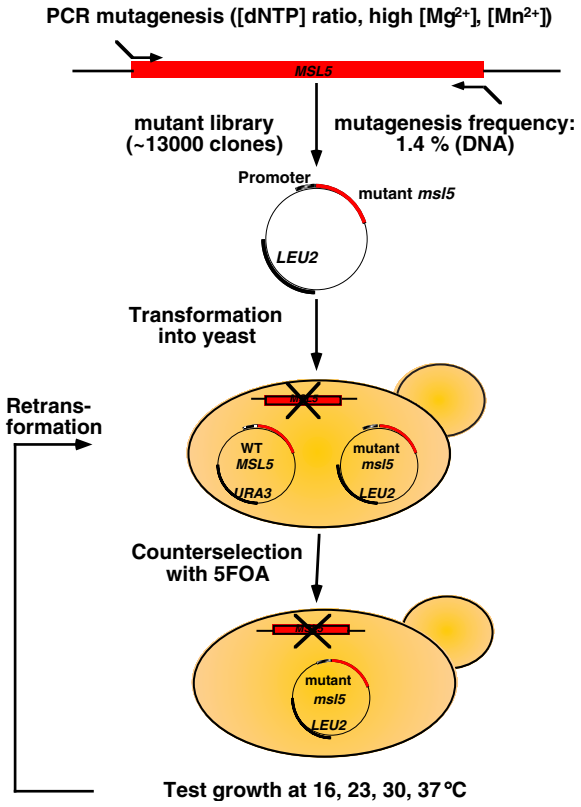

Figure 25. Generation of conditional mutants of *msl5*

Following this selection, 11 clones showed slow or no growth at 37°C (see Figure 26: *msl5-1* to *msl5-4* and *msl5-7* to *msl5-11*, *msl5-13* and *msl5-14*) and one clone showed very slow growth at 16°C (see Figure 26: *msl5-5*) compared to the controls containing *MSL5* on a plasmid (pWT) or on the chromosome (WT). Some of the temperature-sensitive (ts) mutants (*msl5-2*,-3,-4) showed already growth inhibition at 30°C while others (*msl5-11* ,-*14*) were still able to grow with reduced rate at 37°C.

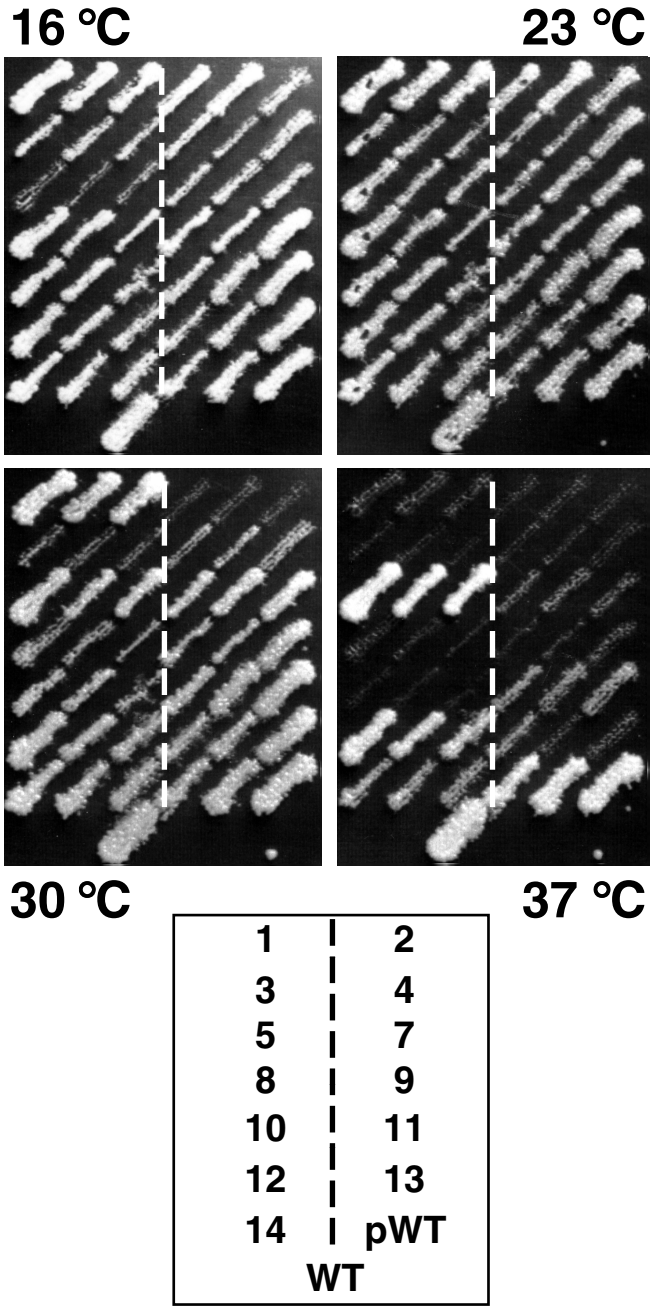

Figure 26. Growth analysis of *msl5* mutants

Three subclones of each mutant and controls containing wild type *MSL5* on a plasmid (pWT) or on the chromosome (WT) were streaked on a plate and grown at 23°C. This masterplate was replicated on plates which were incubated at the indicated temperatures for 3 days (16°C plate for 5 days). Below the pictures the positions of the different mutants and the controls on each plate are indicated by their allele numbers or names.

Quantitative analysis of growth rate in liquid medium confirmed the results obtained on solid medium (Figure 27). For the ts mutants, growth was inhibited at the latest 6 hours after shift to 37°C. For the cs mutant, growth was inhibited 8 hours after shift to the non-permissive temperature (16°C).

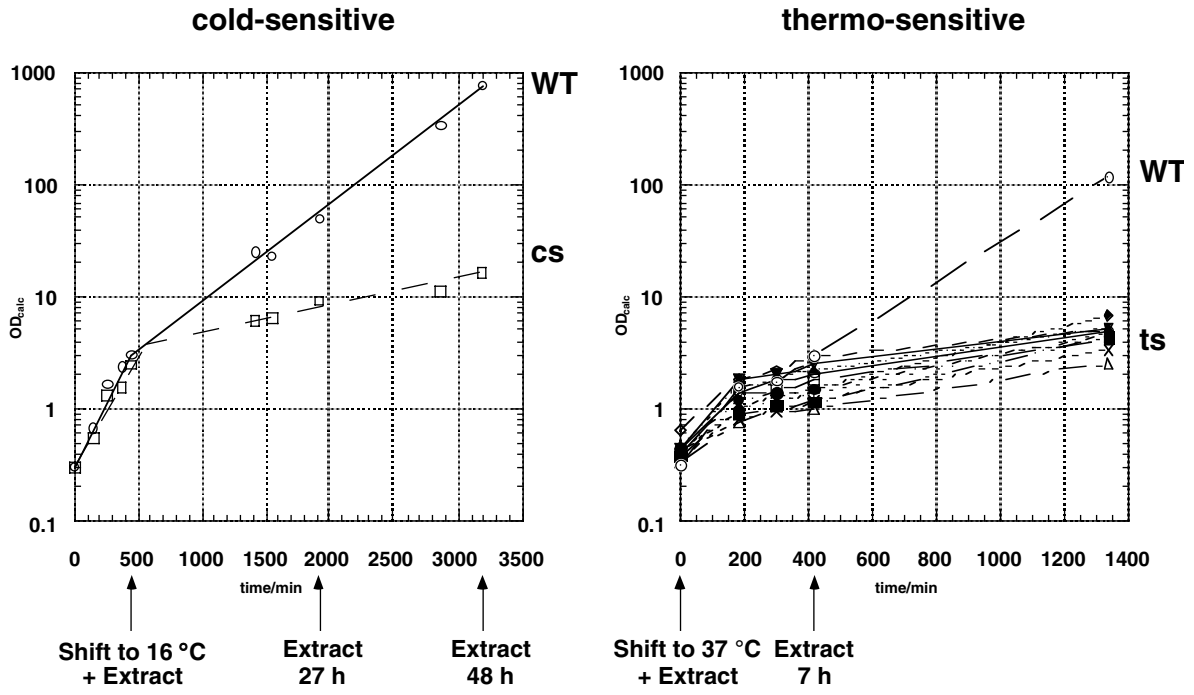

Figure 27. **Growth curve of *msl5* mutants**

The mutant strains and an isogenic control strain containing wild type *MSL5* on a plasmid were grown at the permissive temperature (23°C for the ts mutants and 30°C for the cs mutant). After shift to the non-permissive temperature (37°C for the ts mutants and 16°C for the cs mutant) the incubation was continued and the OD_{600} of the cultures was measured and a cumulative OD_{calc} was calculated (see Materials and Methods). The vertical arrows indicate the removal of aliquots from the cultures for the preparation of extracts.

2.2. Identification of mutations in *msl5-2* (ts) and *msl5-5* (cs)

Because sequencing of several clones (Figure 28) indicated that the mutagenesis procedure had introduced on average 15 amino acid mutations per ORF, we sought to determine the number and the nature of the mutations required for the generation of an *msl5* conditional phenotype.

This analysis revealed a distribution of mutations over the whole ORF length (Figure 28). However, the KH-domain, the STAR-QUA2 domain and the Zn-knuckles seemed to contain less mutations indicating that mutations in these regions might be deleterious for the cell. Two mutants (*msl5-3* and *msl5-4*) seemed to be identical, because the same mutations

were present in both mutants. Most likely these mutants originate from the double cloning of the same PCR product or from a cross-contamination in the selection process.

We selected the strongest ts mutant (*msl5-2*) and the cs mutant (*msl5-5*) for further analysis. The *msl5-2* ORF contained 17 amino acid changes while the *msl5-5* ORF contained 13 amino acid changes (Figure 28). Using standard cloning procedures and three conveniently located restriction sites (*BsmA*I, *Mva1269*I, *Bgl*II), four domains corresponding approximately to the N-terminus, the KH domain, the Zn-knuckle region and the C-terminus (Figure 29) of the *MSL5* ORF were exchanged one by one or in combinations between the mutants and the wild type. The resulting chimeric constructs were reintroduced into yeast and tested for their effect on growth at different temperatures.

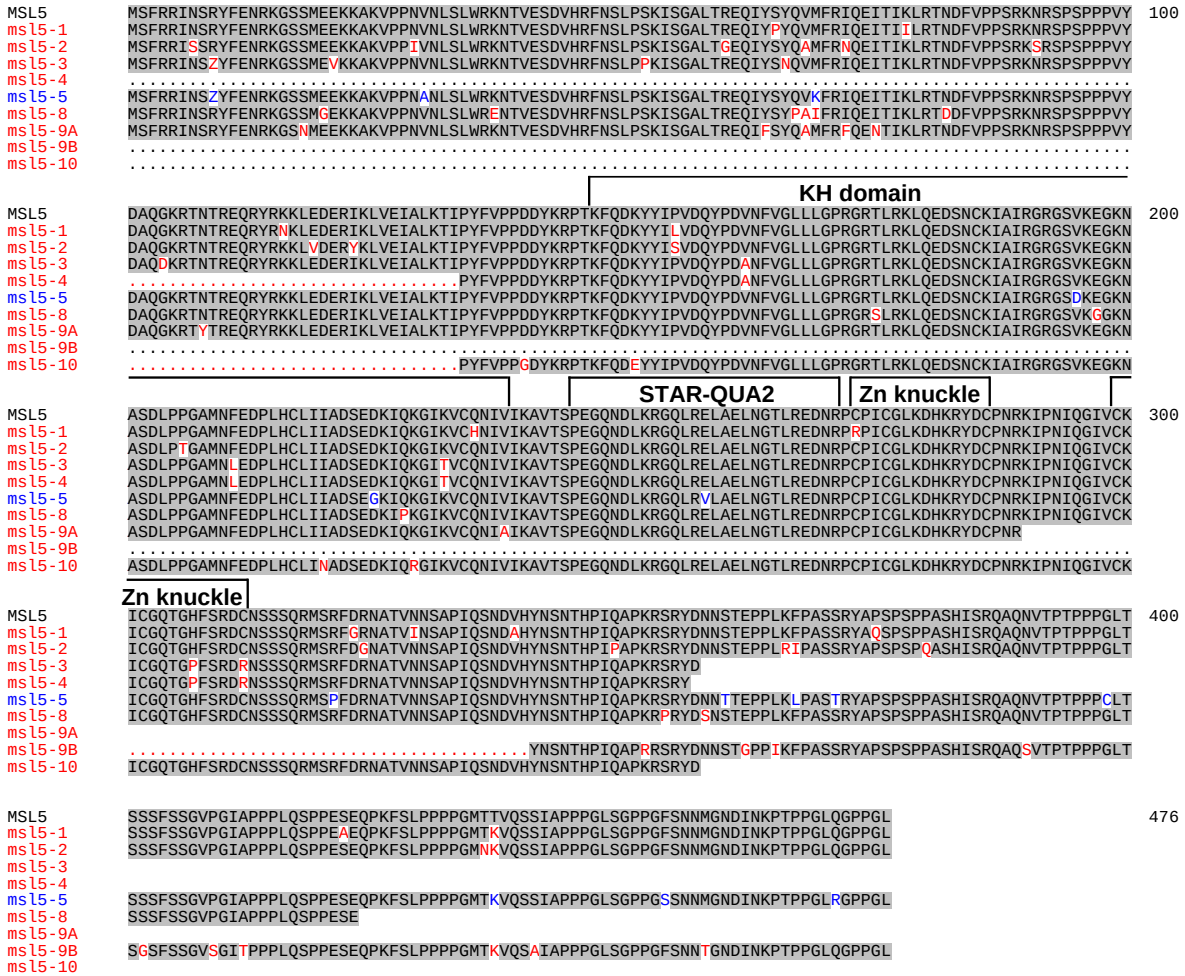

Figure 28. Sequencing of eight *msl5* mutants

The identity of the analyzed mutants (msl5-) and the wild type gene (MSL5-WT) are indicated on the left side of the sequences. The structural domains of BBP/SF1 are shown above the alignment. Mutations are indicated with white background. Note that several mutants were only partially sequenced (msl5-3, msl5-4, msl5-8, msl5-9, msl5-10).

The N- and the KH domain of *msl5-2* were both required to confer the ts phenotype to the otherwise wild type ORF. The KH and the Zn-domain of *msl5-5* were both necessary to retain the cs phenotype. Since the KH domain in both cases contained only a single mutation, this mutation was clearly required for the phenotype (Figure 29). To reduce further the number of mutations, additional constructs that contained different combinations of mutations in addition to the mutation in the KH domain (see Table 1 and Materials and Methods) were generated.

Plasmid	Name	Number of Mutations	12°C	16°C	23°C	30°C	37°C
pBS1759	MSL5-WT	1	+	+	+	+	+
*pBS2082	MSL5-WT rep.	-	+	+	+	+	+
*pBS1811	msl5-2	17	n.a.	+	+	-	-
pBS1892	msl5-2 N+KH+Zn	12+1	n.a.	n.a.	+	-	-
pBS1891	msl5-2 N+KH	9+1	n.a.	n.a.	+	-/+	-
pBS1895	msl5-2 Zn+C	8	n.a.	n.a.	+	+	+
pBS1910	msl5-2 N	8+1	n.a.	n.a.	+	+	+
pBS1911	msl5-2 KH	1+1	n.a.	n.a.	+	+	+
pBS1990	msl5-2 N(n2)+KH	3+1	n.a.	n.a.	+	+	+
pBS1991	msl5-2 N(c6)+KH	7+1	n.a.	n.a.	+	-/+	-
pBS1992	msl5-2 N(n6)+KH	7+1	n.a.	n.a.	+	-/+	-
pBS1993	msl5-2 N(c2)+KH	3+1	n.a.	n.a.	+	+	+
pBS2013	msl5-2 N(m4)+KH	5+1	n.a.	n.a.	+	+	-
no stock	msl5-2 N(#1)+KH	2+1	n.a.	n.a.	+	+	+
no stock	msl5-2 N(#2+3)+KH	3+1	n.a.	n.a.	+	+	+
no stock	msl5-2 N(#2+3+4)+KH	4+1	n.a.	n.a.	+	+	+
no stock	msl5-2 N(#1+4)+KH	3+1	n.a.	n.a.	+	+	+
no stock	msl5-2 N(#4)+KH	2+1	n.a.	n.a.	+	+	+
no stock	msl5-2 N(#1+2)+KH	3+1	n.a.	n.a.	+	+	+
pBS2012	msl5-2 N(#1+2+3)+KH	4+1	n.a.	n.a.	+	+	-/+
pBS2078	msl5-2 N(#1+3)+KH	3+1	n.a.	n.a.	+	+	-/+
*pBS2083	msl5-2 N+KH rep.	9	n.a.	n.a.	+	-/+	-
*pBS2084	msl5-2 N(n6)+KH rep.	7	n.a.	n.a.	+	-/+	-
*pBS2085	msl5-2 N(#1+2+3)+KH rep.	4	n.a.	n.a.	+	+	-/+
*pBS2086	msl5-2 N(#1+3)+KH rep.	3	n.a.	n.a.	+	+	-/+
*pBS1814	msl5-5	13	-	-	+	+	+

pBS1883	msl5-5 N+KH	4+1	n.a.	+	+	n.a.	n.a.
pBS1884	msl5-5 N+KH+Zn	6+1	n.a.	-/+	+	n.a.	n.a.
pBS1896	msl5-5 KH	1+1	n.a.	+	+	n.a.	n.a.
pBS1912	msl5-5 Zn	2+1	n.a.	+	+	n.a.	n.a.
pBS1975	msl5-5 KH+Zn	3+1	n.a.	-/+	+	n.a.	n.a.
pBS1976	msl5-5 N+Zn	5+1	n.a.	+	+	n.a.	n.a.
pBS1988	msl5-5 KH+Zn(n1)	2+1	+	+	+	n.a.	n.a.
pBS1989	msl5-5 KH+Zn(c1)	2+1	-/+	+	+	n.a.	n.a.
*pBS2087	msl5-5 N+KH+Zn rep.	6	-	-/+	+	n.a.	n.a.
*pBS2088	msl5-5 KH+Zn(c1) rep.	2	-/+	+	+	n.a.	n.a.

Table 1. Mutation mapping in *msl5-2* and *msl5-5*
Growth of strains containing the different constructs as the only source of BBP/ScSF1 was tested at different temperatures on YPD plates (+: wild type growth, -: no growth, -/+: slow growth, n.a.: not analyzed). The star (*) before the plasmid number indicates the constructs used in Figure 31.

The final construct contained the minimal number of mutations required for generating a conditional phenotype. For *msl5-2*, two mutations were required in the N-domain (R60→G, I72→N) and one mutation in the KH domain (P155→S). For the *msl5-5* mutant the mutation E258→V was found to be required together with the mutation V195→D in the KH domain to confer the cs phenotype (Figure 29).

In the sequencing of the minimal mutant constructs a point mutation (T437→K) was identified that had so far escaped detection because it was present also in the wild type construct which had been used to generate all conditional mutants and many of the mapping constructs. This point mutation was most likely due to a PCR mistake in the initial amplification of the *MSL5* ORF and had therefore been transferred to all mutants and mapping constructs. However, repair of this point mutation by domain swapping with another wild type construct (pBS1703, see Materials and Methods) revealed that it had no effect on growth at all temperatures tested (Table 1, compare pBS1759 with pBS2082). Several constructs that had been tested before where checked again after removal of this mutation (indicated with “rep.” after the name, see Table 1 and Materials and Methods). No influence of this point mutation on the growth phenotype was observed (Table 1).

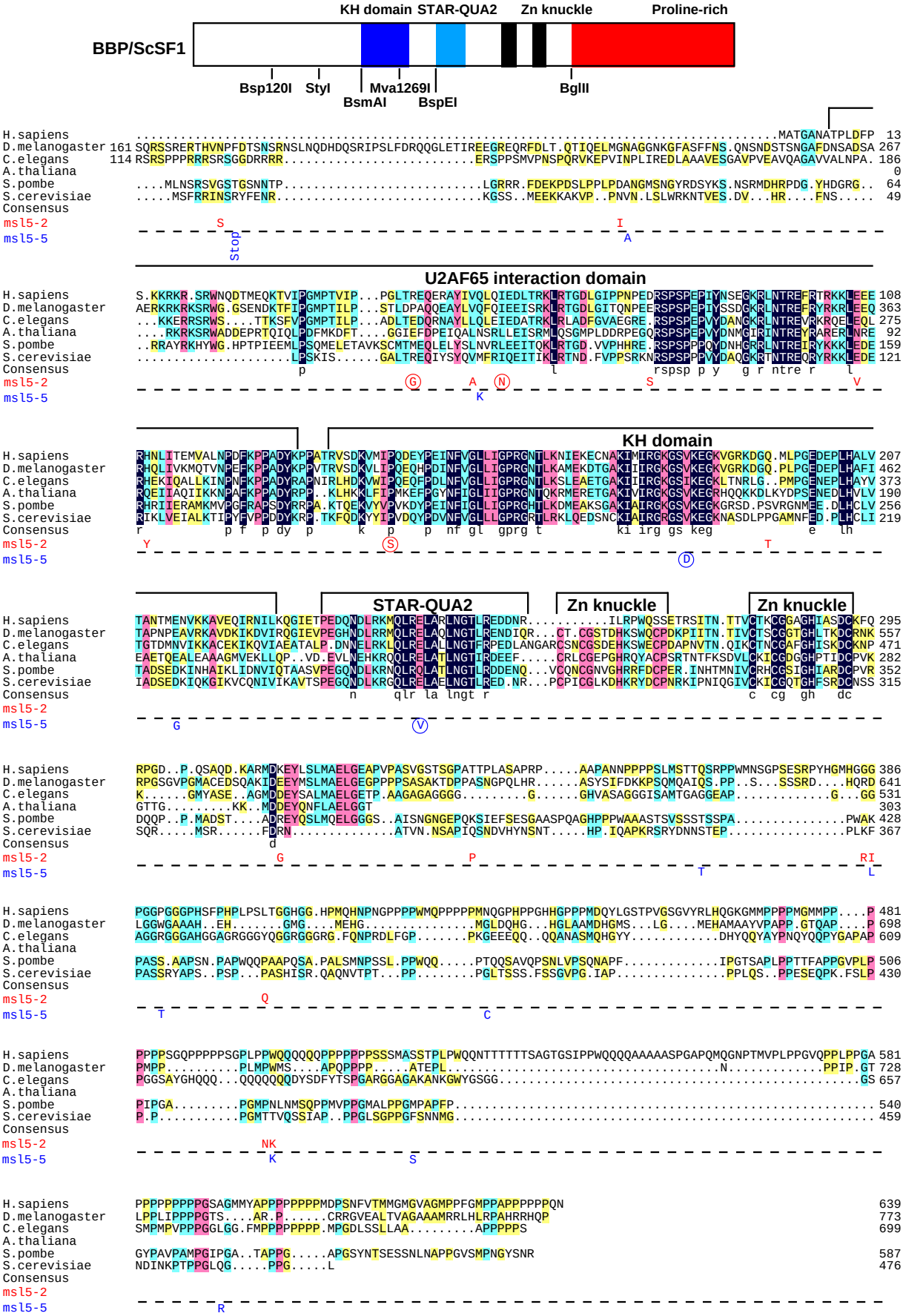
KH domain
STAR-QUA2
Zn knuckle
Proline-rich
BBP/ScSF1
Bsp120I
StyI
Mva1269I
BsmAI
BspEI
BglII
U2AF65 interaction domain
KH domain
STAR-QUA2
Zn knuckle
Zn knuckle
H.sapiens
D.melanogaster
C.elegans
A.thaliana
S.pombe
S.cerevisiae
Consensus
msl5-2
msl5-5
Stop

Figure 29 (previous page). Amino acid sequence alignment of SF1 orthologs and position of mutations in *msl5-2* and *msl5-5*

Putative homologues of SF1 from *H. sapiens*, *D. melanogaster*, *C. elegans*, *A. thaliana* (partial sequence), *S. pompe* and *S. cerevisae* were aligned using the program ClustalX (Thompson *et al*., 1997) and manual refinement. Amino acids are shaded according to the degree of conservation. Functional domains and structural motifs are indicated above the alignment. The U2AF^{65} interaction domain is drawn according to the results published for HsSF1 (Rain *et al*., 1998). The position of point mutations in the cs mutant *msl5-5* (below the dashed line) and in the ts mutant *msl5-2* (above the dashed line) are indicated below the *S. cerevisiae* SF1 sequence. Mutations that were sufficient and necessary to retain a growth defect are encircled (compare with Figure 31). Sequences have the following accession numbers: AtSF1, AB023044, CeSF1, AJ243905, DmSF1, AJ243904, HsSF1, Y08765, ScSF1, U53877, SpSF1, SPTREMBL O74555. The partial protein sequence of *A. thaliana* SF1 was generated by comparison of the genomic sequence with a profile (derived from an alignment of the known SF1 orthologues with the program PROFILEWEIGHT, Thompson *et al*., 1994) using the program PairWise (Birney *et al*., 1996). Restriction enzymes used for domain swapping between mutants and wild type ORFs are shown below the cartoon on top which depicts the structural organization of BBP/ScSF1.

The sequence alignment shown in Figure 29 was used to generate a secondary structure prediction for BBP/SF1. Only the conserved region (aa 50-325 in the *S. cerevisiae* protein) was chosen for this analysis

The prediction revealed that the mutations R60→G and I72→N in *msl5-2* are in a region that has high probability to be helical. The mutation P155→S in *msl5-2* is located at the end of a proposed β-strand. The mutation V195→D in *msl5-5* lies in a unstructured flexible loop, while E258→V is situated in an α-helix (Figure 30).

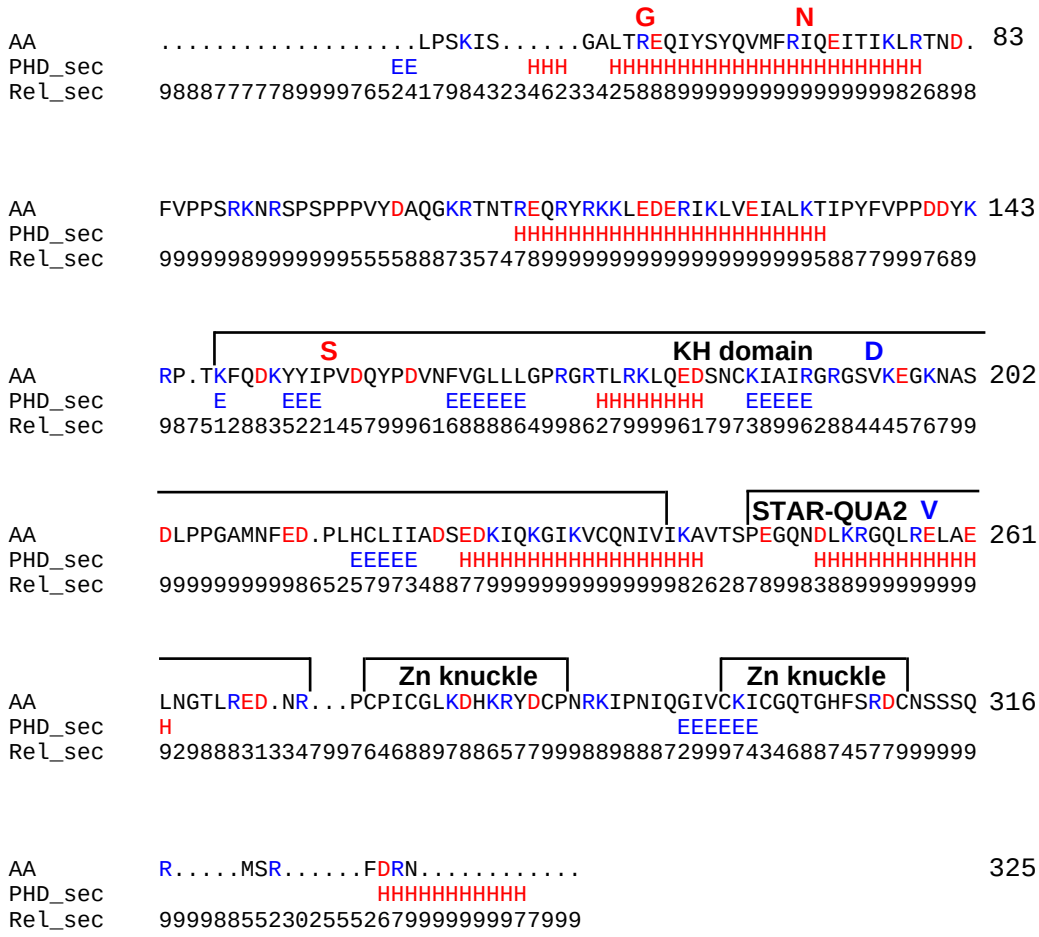

Figure 30. Secondary structure prediction for BBP/SF1

The program PREDICT was used to create a secondary structure prediction of an alignment of the SF1 family. Only the conserved part of the protein (aa 50-325 in the *S. cerevisiae* protein) was included. The different structural domains and the most important mutations in *msl5-2* (red) and *msl5-5* (blue) are indicated above the sequence. PHD_sec: PHD predicted secondary structure: H=helix, E=extended (sheet), blank=other (loop); rel_sec: reliability index for PHDsec prediction (0=low to 9=high).

The growth analysis shown in Figure 31 was performed with the repaired constructs that did not contain the point mutation T437→K (except for the original mutant constructs, *msl5-2* and *msl5-5*). For both mutants *msl5-2* and *msl5-5*, the reduction in the number of mutations was found to reduce the severity of the growth defect, e.g. while the original *msl5-2* mutant was barely growing at 30°C the final mutant containing only three point mutations was nearly wild type at 30°C and showed residual growth at 37°C (Figure 31). Similarly, the original cs mutant was cold-sensitive at 16°C while the mutant containing only two point mutations showed still very slow growth at 12°C (Figure 31).

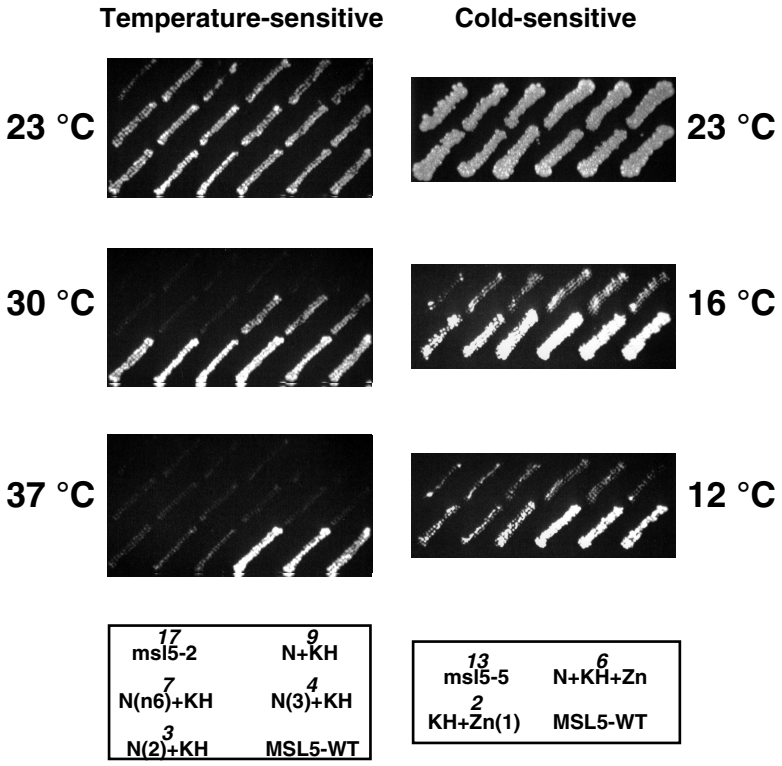

Figure 31. Growth analysis of minimal mutants derived from *msl5-2* and *msl5-5*

Partial mutants of *msl5-2* (ts) and *msl5-5* (cs) were generated by domain swapping between the original mutants and the wild type or by site directed generation of mutations by PCR. Mutant derivatives were compared with the original mutants (*msl5-2* or *msl5-5*) and the wild type (*MSL5*-WT) for their growth at different temperatures (as indicated on side of the plates). The names of the different mutant derivatives and the number of mutations (in italics) are indicated in the cartoon below in the same position as on the replica plates. Three subclones of each strain are shown side by side.

This indicates that the combination of several mutations accounts for the observed strong phenotype. This may explain why *MSL5* has so far escaped genetic screens for conditional mutants affecting splicing (Hutchison *et al*., 1969; Vijayraghavan *et al*., 1989; Noble and Guthrie, 1996). Indeed, accumulation of such a large number of mutations is very unlikely to be achieved with classical mutagenesis techniques.

In summary, we could show that several amino acid mutations are required for the strong growth phenotype of two *msl5* mutants. The most relevant mutations were located in evolutionary conserved domains of the protein.

2.3. Temperature-sensitive mutants of *msl5* show no effect on (pre)-spliceosome formation and *in vitro* splicing

The temperature-sensitive *msl5* mutant strains and an isogenic wild type control strain (BSY809) containing *MSL5* on a plasmid were grown at permissive temperature (23°C) and equal numbers of cells were removed before and 6 hours after a temperature shift to 37°C. Splicing extracts were prepared and analyzed for the formation of splicing complexes and for *in vitro* splicing. To test for commitment complex formation, extracts were incubated with labeled pre-mRNA in the absence of ATP. The resulting complexes were analyzed by native gel electrophoresis (Séraphin and Rosbash, 1989). Extracts from the mutant cells

grown at the permissive temperature were blocked in CC2 formation and accumulated CC1 (Figure 32A, lanes 1-4 and 7-14), while the wild type control (WT) showed normal levels of CC2 (Figure 32A, lane WT). The same result was obtained for extracts prepared from cells grown at non-permissive temperature (Figure 32B). This result confirmed that BBP/ScSF1 has a crucial role for the formation of CC2. Furthermore, this demonstrated that even very weak mutants that showed only little growth defect at 37°C and no growth defect at 30°C (like *msl5-11* and *-14*, Figure 26) were already blocked in CC2 formation at the permissive temperature (Figure 32A).

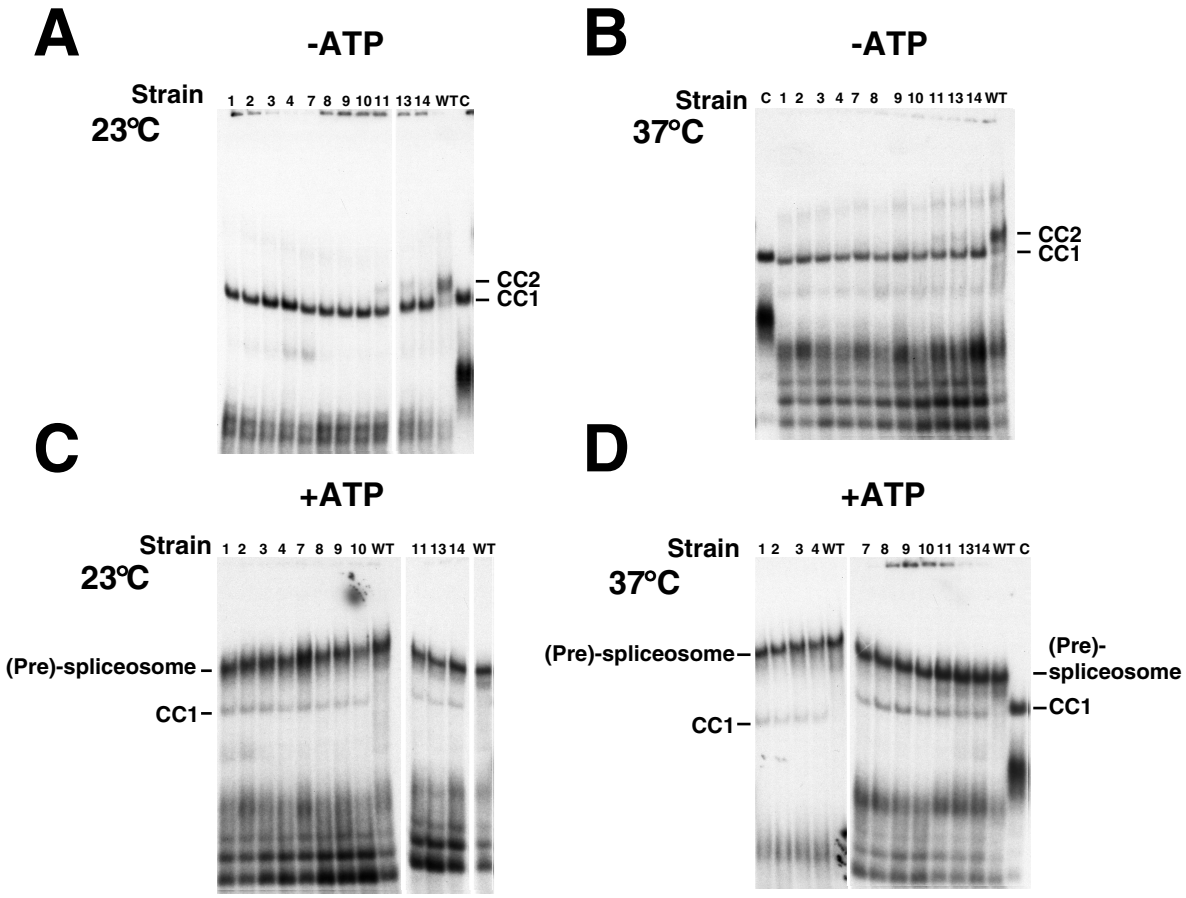

Figure 32. Splicing complex analysis of temperature-sensitive mutants

Extracts from cells grown at permissive (23°C) or non-permissive (37°C) temperature were incubated with labeled pre-mRNA for 30 min at 30°C in the absence (-) or presence (+) of ATP. The resulting complexes were analyzed in native gels. The allele number of the corresponding mutant strain or the wild type control (WT) is indicated above each lane. A control reaction was performed with the wild type extract and a labeled pre-mRNA lacking the branchpoint sequence (C) to obtain a marker for the migration of CC1
Note that the wild type extract used in lane C was prepared with a different method (Newman, 1994), which yields more concentrated extracts. This results in a slight retardation of the migration of CC1 and of the unspecific complex in the lower part of the gel.

(Pre)-spliceosome assembly was assayed by gel electrophoresis after incubation at 30°C in the presence of ATP. At the non-permissive temperature, it was not possible to perform the complex assembly assays because aggregates formed that were not resolved in the native gel (data not shown). The levels of (pre)-spliceosome were not reduced in the mutant strains compared to the wild type for both growth temperatures (Figure 32C and D). However, for both temperatures, reactions with the mutant extracts contained an additional complex, which was absent in reactions containing the wild type extract. This complex comigrated with CC1 (Figure 32D, compare with the marker in lane C). It is noteworthy that a similar phenotype has been observed following biochemical and/or genetic depletions of BBP/ScSF1 (Figure 20, Figure 21). To test whether (pre)-spliceosomes assembled in the mutant extracts were functional, we analyzed intermediates and products of *in vitro* splicing reactions containing an RP51A intron substrate by denaturing gel electrophoresis. These reactions were performed at 25°C because *in vitro* splicing was inhibited at higher temperatures already for the wild type extract (data not shown). Comparison with a wild type extract showed variability in the efficiency of *in vitro* splicing for some mutants at the non-permissive temperature (Figure 33, e.g. *msl5-1*0), while at 23°C no significant differences could be observed. Because the quality of the individual extracts has a strong influence on the resulting splicing activity (Cheng *et al*., 1990) it is not possible to draw quantitative conclusions from this experiment (e.g. note that several mutants with a strong growth defect, like *msl5-2*, were not reduced in splicing efficiency). However, qualitatively, it is striking that all mutant extracts were able to splice an exogenous reporter pre-mRNA.

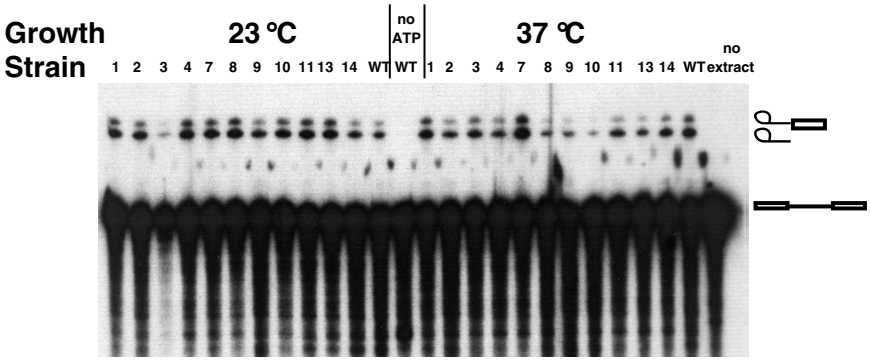

Figure 33. *In vitro* splicing analysis of temperature-sensitive mutants

Extracts from cells grown at permissive (23°C) or non-permissive (37°C) temperature were incubated with labeled pre-mRNA for 30 min at 25°C in the presence of ATP. RNA was extracted and analyzed in a denaturing gel. The allele number of the corresponding mutant strain or the wild type control (WT) is indicated above each lane. Control reactions in the absence of ATP (no ATP) or extract (no extract) were analyzed in parallel. The observed RNA species (from top to bottom: lariat intermediate, intron lariat, pre-mRNA) are indicated by cartoons on the side. Exon 1 and mRNA were obscured by degradation products from the pre-mRNA.

Overall, these analyses demonstrated a role of BBP/ScSF1 in CC2 formation, but failed to indicate an effect of the ts mutations on (pre)-spliceosome assembly or activity. These results are consistent with, and confirm, the results obtained following depletion of this factor (see 1.). Moreover, the analysis of 11 independent mutants showed that this phenotype is related to the function of BBP/ScSF1 and is not allele-specific or due to limitations of the depletion methods.

2.4. Cold sensitive mutant of *msl5* blocks (pre)-spliceosome formation at non-permissive temperature

The cold-sensitive mutant (*msl5-5*) was grown together with the isogenic wild type strain (BSY809) at permissive temperature (30°C) and cells were collected before and 27 hours after a temperature shift to 16°C. Extracts were prepared from the different samples. For the analysis of commitment complex formation, extracts were incubated with labeled pre-mRNA substrate in the absence of ATP. The incubation temperature was identical to the temperature of previous growth. At both temperatures a block in CC2 formation and accumulation of CC1 were observed for the mutant while the wild type showed normal levels of CC2 (Figure 34A, compare lanes 2, 4 and lanes 3, 5). This was similar to the phenotype observed for the ts mutants.

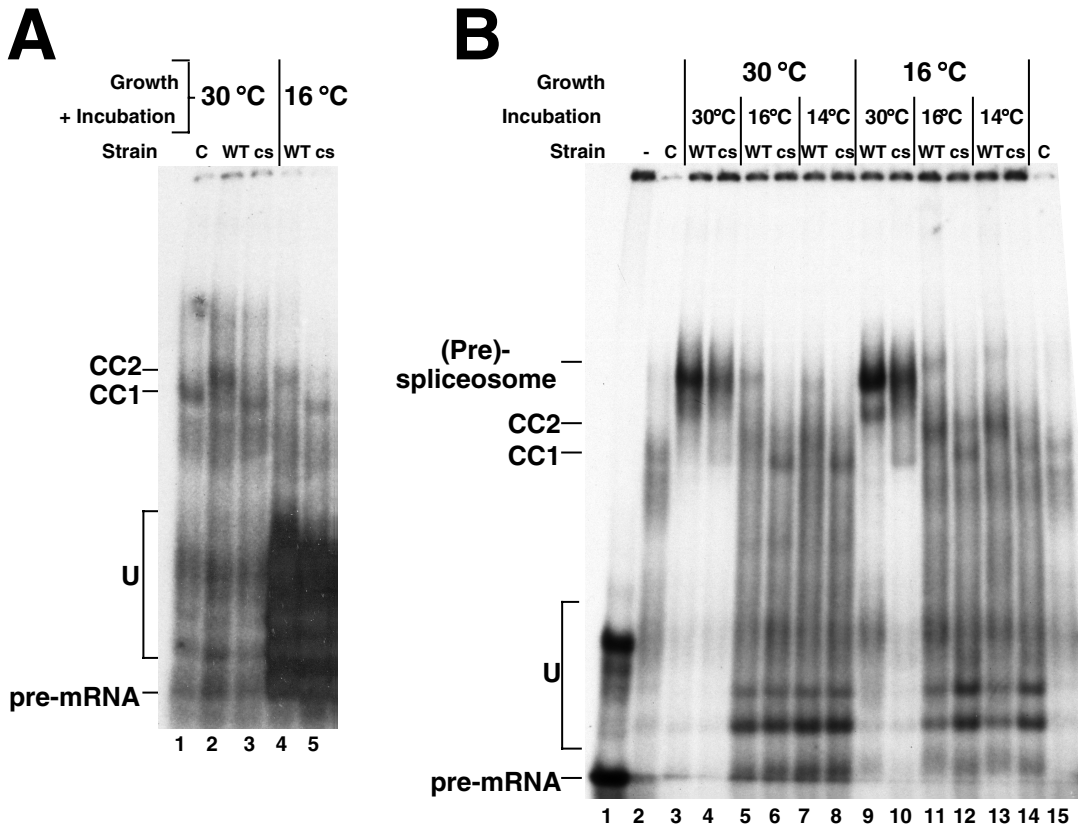

Figure 34. Splicing complex analysis of cold-sensitive mutant

A: Commitment complex analysis of the cold-sensitive mutant. Extracts from cells grown at permissive (30°C) or non-permissive (16°C) temperature were incubated with labeled pre-mRNA for 30 min at 30°C or 16°C in the absence of ATP. Reactions containing extracts from the mutant strain (cs) or the wild type control (WT) are indicated above each lane. A control reaction was performed with the wild type extract and a labeled pre-mRNA lacking the branchpoint sequence (C) to obtain a marker for the migration of CC1.
B: (Pre)-spliceosome analysis of cold sensitive mutant. Extracts from cells grown at permissive (30°C) or non-permissive (16°C) temperature were incubated with labeled pre-mRNA for 30 min at 30°C, 16°C or 14°C in the presence of ATP. Labeling of the gel is like in panel A.

To analyze (pre)-spliceosome formation, we performed assembly reactions at three different incubation temperatures (30°C, 16°C and 14°C) for the extracts from cells grown at permissive and at non-permissive temperature. We observed nearly identical patterns for both growth temperatures (Figure 34B, compare lanes 3-8 and 9-14). In both cases slightly reduced levels of (pre)-spliceosome were observed for the cs mutant when the extracts were incubated at 30°C (Figure 34B, compare lanes 3 and 4, 9 and 10). However, when the incubation was performed at 16 or 14°C (pre)-spliceosome formation was abolished in the mutant extracts while the wild type extracts showed significant, but strongly reduced levels of (pre)-spliceosomes (Figure 34B, lanes 5-8 and 11-14). As already observed in the analysis of commitment complexes and also for the ts mutants, CC1 accumulated at the non-permissive temperature in the mutant strains. In contrast, the wild type strain showed

some accumulation of CC2 in addition to (pre)-spliceosomes at the low temperatures (Figure 34B, lanes 5, 7, 11, 13).

This experiment revealed that the cs mutant of *msl5*, in contrast to the ts mutants, shows a block of (pre)-spliceosome formation that can be induced *in vitro* and does not depend on the prior growth temperature of the cells.

We tested the activity of the extracts for splicing *in vitro* at two different temperatures (25 and 16°C). Surprisingly, we could not observe any difference in splicing comparing mutant with wild type extracts (Figure 35). This suggests that a low level of mature spliceosomes can still assemble and that the complexes seen *in vitro* are not rate limiting for the formation of spliced products.

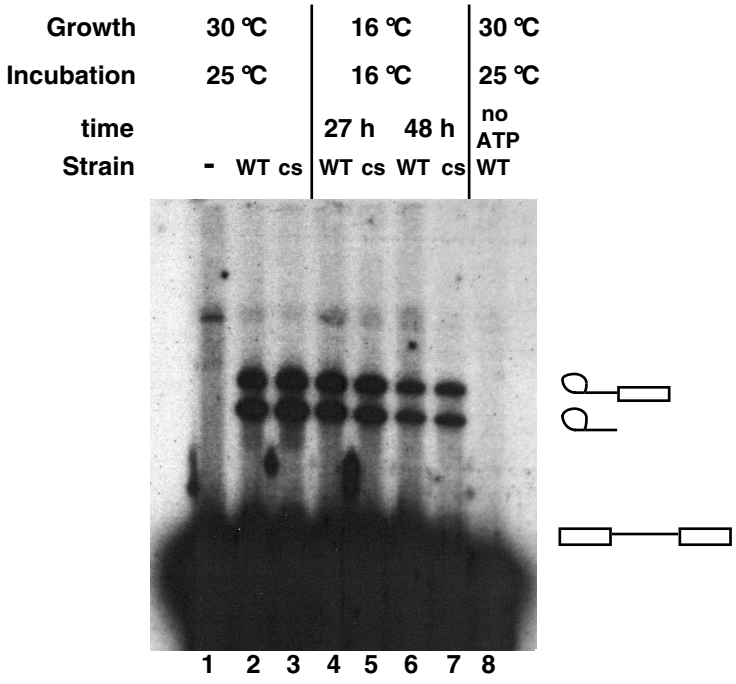

Figure 35. *In vitro* splicing analysis of the cold-sensitive mutant

Extracts from cells grown at permissive (30°C) or non-permissive (27 or 48 h at 16°C) temperature were incubated with labeled pre-mRNA for 30 min at 25°C or 16°C in the presence of ATP. RNA was extracted and analyzed in a denaturing gel. The mutant strain (cs) or the wild type control (WT) are indicated above each lane. Control reactions in the absence of ATP (no ATP) or extract (-) were analyzed in parallel. The observed RNA species (from top to bottom: lariat intermediate, intron lariat, pre-mRNA) are indicate by cartoons on the side. Exon 1 and mRNA were obscured by degradation products from the pre-mRNA.

This extends our observation of a block in CC2 formation and no significant defects in *in vitro* splicing to the cs mutant. However, the cs mutant, in contrast to the ts mutants, showed a defect in (pre)-spliceosome formation or stability at the non-permissive temperature.

2.5. Conditional mutants of *msl5* are affected in the splicing of weak introns *in vivo* and show increased pre-mRNA leakage to the cytoplasm

Three ts mutants (*msl5-2*,-3,-9) and the cs mutant (*msl5-5*) were selected to analyze their *in vivo* effects on splicing and pre-mRNA leakage. Two different reporter systems were used (Figure 36): for the analysis of subtle splicing defects, reporters containing the RP51A intron or mutants thereof inserted within the reading frame of the lacZ gene (Teem and Rosbash, 1983; Jacquier *et al*., 1985) were utilized. For the analysis of pre-mRNA leakage, a set of synthetic introns designed in a way that either the pre-mRNA or the mRNA codes for β-galactosidase was employed (Legrain and Rosbash, 1989). This last system allows for the detection of pre-mRNAs that have been exported to the cytoplasm where they are translated (Figure 36).

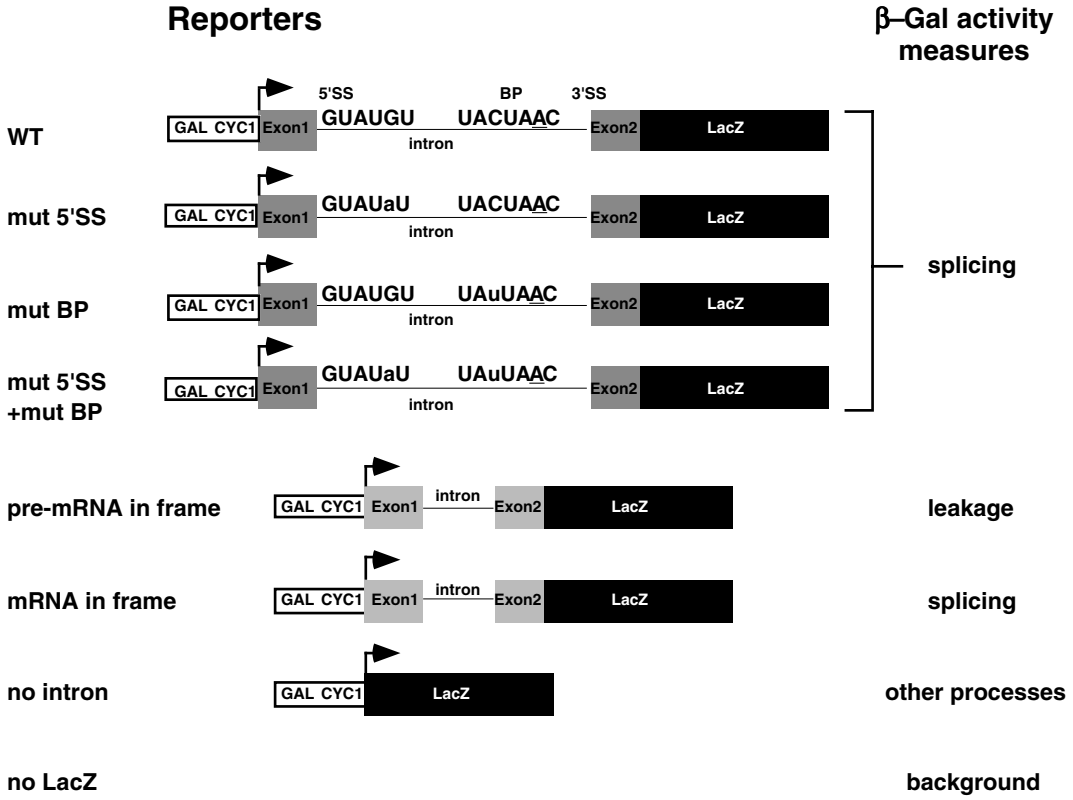

Figure 36. Reporter system for analysis of splicing and pre-mRNA leakage

The names of the reporters are indicated on the left. Conserved residues forming the splice sites and the branchpoint are shown in capital letters, mutations are shown in small letters. The branchpoint residue is underlined. The promoter of the reporters is indicated as a white box (GAL Cyc1). Exons and the LacZ gene are shown as gray and black boxes, introns are shown as black lines.

The *msl5* mutant strains and an isogenic wild type strain transformed with these reporters were assayed for β-galactosidase activity after induction of the reporter and incubation at

the non-permissive temperature for 2 h (ts) or 4 h (cs). This revealed only a two-fold decrease in the splicing of the RP51A intron in the ts mutants (Figure 37A, WT-intron). However, splicing of introns containing a mutated 5' splice site (mut5'SS) or a mutated branchpoint region (mutBP) or the combination of both was much more affected comparing the mutant strains to the wild type (10-100-fold for mut5'SS, Figure 37A). The difference in splicing efficiency observed for the three *msl5* mutants correlated well with the severity of their respective growth defects (Figure 37A mut5'SS, mutBP and Figure 26). This observation could be partly extended to the other mutants (Figure 39).

For a more sensitive analysis of the splicing phenotype, RNA was extracted from the three mutants and an isogenic wild type strain after induction of the RP51A derived reporters as described above. Primer extension was performed with a primer complementary to exon 2 of both the reporter and the endogenous RP51A gene. All BBP/ScSF1 mutants showed a decrease in splicing efficiency for the mutant 5' splice site and mutant branchpoint containing reporters as judged by the decrease in mRNA levels and accumulation of pre-mRNA (Figure 38). This was verified by quantitative analysis of the gel and calculation of the mRNA/pre-mRNA ratio (Figure 38, bottom), the best indicator of splicing efficiency (Pikielny and Rosbash, 1985). While the wild type intron was spliced only slightly less efficient in the mutants than in the wild type (1.5 to 3-fold decreased), the decrease in splicing efficiency was obvious for the reporters containing mutations in the splice sites (about 10-fold in the 5' splice site mutant). As already observed for the β-galactosidase activity, the severity of the mutant phenotypes correlated with the defect in splicing efficiency (compare *msl5-2* and *msl5-9*). This demonstrates that BBP/ScSF1 is involved in the splicing of introns *in vivo*, but indicates that this function is more pronounced for the splicing of introns with weak consensus splice sites. Furthermore, this is consistent with the lack of phenotype of the *in vitro* splicing analysis performed with the wild type RP51A intron (Figure 33).

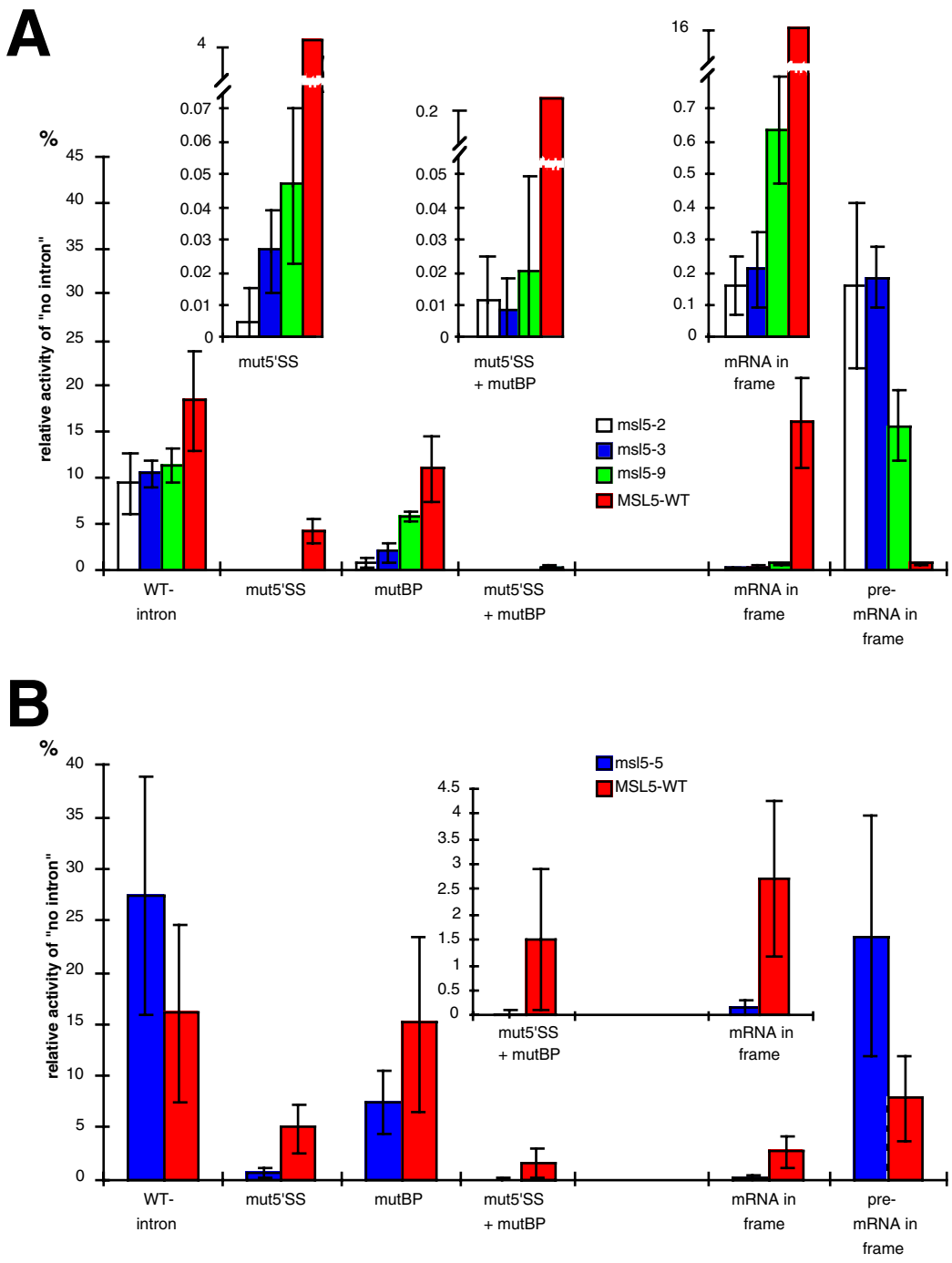

Figure 37. Splicing and pre-mRNA leakage analyses

A: Temperature-sensitive mutants *msl5-2*, *-3* and *-9*. The reporters contained the RP51A intron in the wild type form (WT-intron) or with a mutation in the 5' splice site (mut5'SS), in the branchpoint (mutBP) or in both (mut5'SS+mutBP) interrupting the reading frame of the *lacZ* gene. Another set of reporters contained a synthetic intron, which was designed in a way that either the mRNA (mRNA in frame) or the pre-mRNA (pre-mRNA in frame) would code for β-galactosidase. Activity is expressed as the relative β-galactosidase activity of a construct containing no intron in the *lacZ* gene. The insets show enlarged details of the plots where necessary (note the different scales).

B: Cold sensitive mutant *msl5-5*. The analysis was performed as in A, but cells were grown at 30°C, transferred for 30 min at 16°C before induction for 4 hours at 16°C.

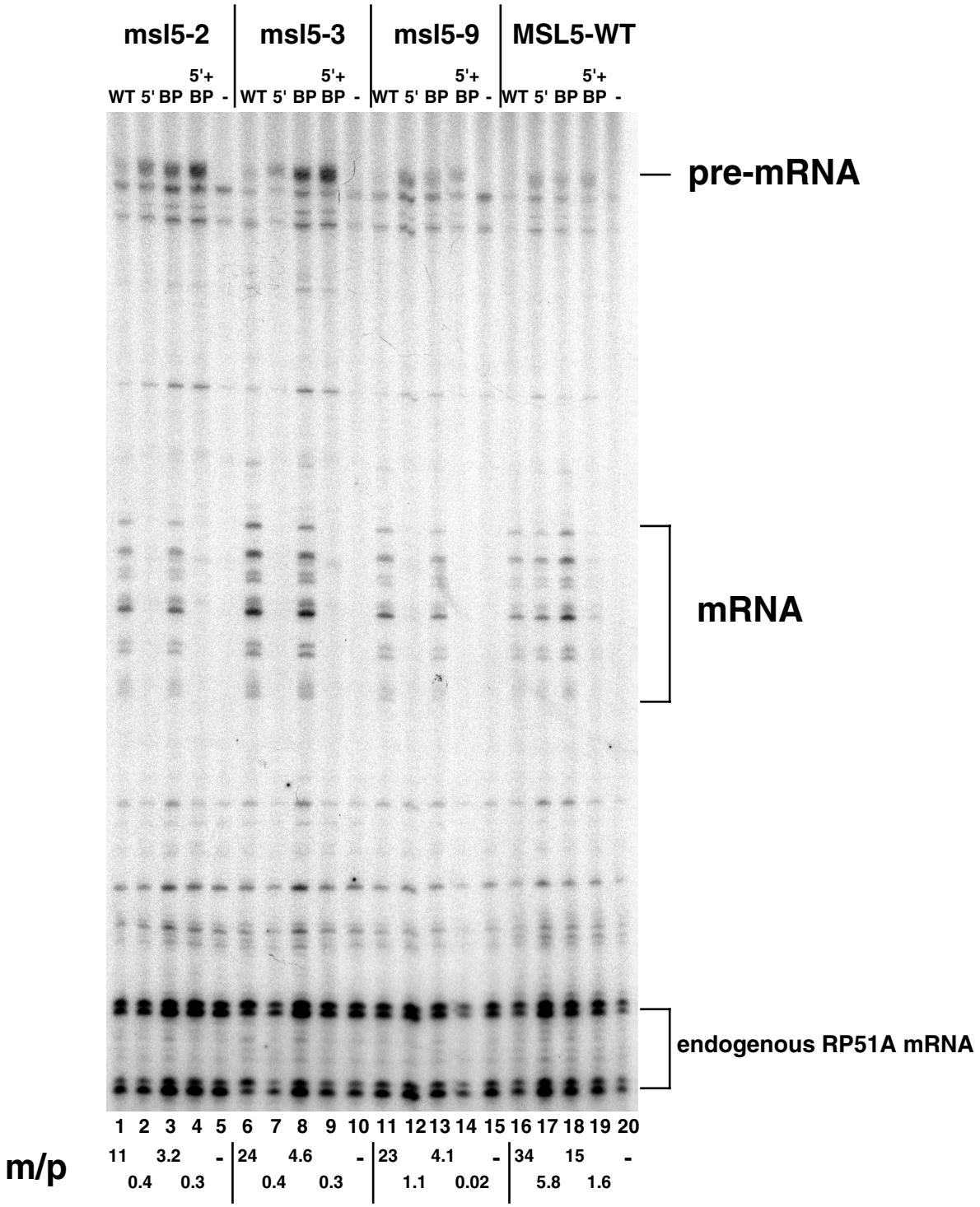

Figure 38. Primer extension analysis

RNA was extracted from cells that had been treated as described for Figure 37. The reporters used contained the RP51A intron in the wild type form (WT), with a mutation in the 5' splice site (5'), in the branchpoint region (BP) or in both (5'+BP). As a control for the background from endogenous RNA, cells containing an empty vector (-) were analyzed. The signals corresponding to pre-mRNA and mRNA were quantified and the ratio of mRNA/pre-mRNA (m/p) is plotted below each lane.

The second set of reporters was used to analyze the effect of BBP/ScSF1 activity on pre-mRNA leakage to the cytoplasm. Strikingly, a 20- to 40-fold increase in leakage of the pre-mRNA to the cytoplasm was detected in the mutants at the non-permissive temperature (Figure 37A, pre-mRNA in frame). This reveals a role for BBP/ScSF1 in nuclear pre-mRNA retention. The large increase of pre-mRNA export was accompanied by a strong reduction of pre-mRNA splicing of the reporter (Figure 37A, mRNA in frame). The reduction of pre-mRNA splicing observed with this reporter is consistent with our conclusion that BBP/ScSF1 particularly affects splicing of introns that are inefficiently spliced (see above), as reported for the intron in these constructs (Legrain and Rosbash, 1989). Again, the severity of the splicing and pre-mRNA leakage phenotype correlated well with the growth defects of the different mutants (Figure 37A, Figure 26). This observation could be partially extended to the remaining eight ts mutants (Figure 39). However, since the error of these measurements is quite high and the experiment was only performed once, not all results were conclusive (for example WT-intron in *msl5-8*).

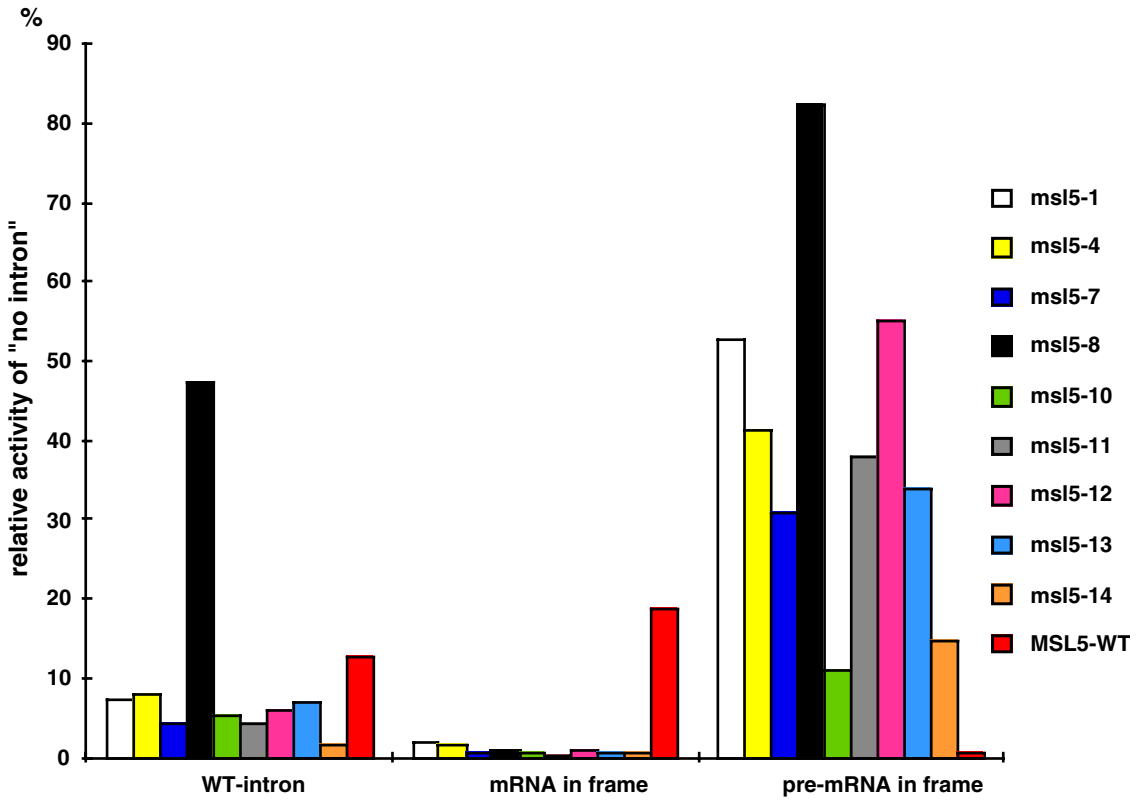

Figure 39. Splicing and pre-mRNA leakage analyses of *msl5-1,-4,-7,-8,-10,-11,-12,-13,-14*

The analysis was performed as in Figure 37A. The reporters contained the RP51A intron in the wild type form (WT-intron) or a synthetic intron, which was designed in a way that either the mRNA (mRNA in frame) or the pre-mRNA (pre-mRNA in frame) would code for β-galactosidase. Acitivity is expressed as the relative activity of a construct containing no intron in the *lacZ* gene.

Analysis of the cs mutant showed no significant effect on splicing of the RP51A intron (Figure 37B). However, splicing of reporters containing mutant versions of this intron was significantly reduced (Figure 37B, mut5'SS, mutBP, mut5'SS+mutBP). This confirmed the observations made in the ts mutants. Splicing of the reporter containing the inefficient synthetic intron was also severely inhibited (Figure 37B, mRNA in frame). In the pre-mRNA leakage assay the cs mutant showed an about three-fold increase compared to the wild type (Figure 37B, pre-mRNA in frame). However, the wild type strain also showed an increase in pre-mRNA leakage when compared to the 37 °C experiment (compare Fig. 6A, B). This could indicate that pre-mRNA retention is less stringent at lower temperatures. Consistent with this hypothesis, a strain disrupted for *mud2*, which is known to show increased pre-mRNA leakage, has significantly reduced growth rate at 12 and 16°C compared to a wild type strain (data not shown).

Taken together, the cs mutant had a similar phenotype as the ts mutants, but seemed to be more similar to the intermediate strength ts mutants (like *msl5-9*). This is in agreement with the growth assay, where the cs mutant still grew very slowly at 16°C while most ts mutants did not grow at 37°C (Figure 26).

In summary, analysis of the conditional mutants of *MSL5* revealed two major phenotypes: first, an increase in the leakage of pre-mRNA to the cytoplasm and second, a decrease in splicing efficiency of introns with non-consensus splice sites. This phenotype was observed for all 12 mutants, although the strength of the defect in splicing and pre-mRNA leakage was varying between individual mutants. The defects in splicing and leakage correlated well with the respective growth phenotypes.

2.6. Disruption of *MUD2* shows effect on splicing of non-consensus introns *in vivo* and a minor increase in pre-mRNA leakage to the cytoplasm

The *MUD2* gene, which functions together with *MSL5* in the formation of CC2 (Abovich *et al*., 1994), also seems to be involved in pre-mRNA retention in the nucleus (Rain and Legrain, 1997). However, since *MUD2* is not essential for yeast viability we were expecting that the splicing and leakage defects of a *mud2*-Δ mutant would be less pronounced than for the *msl5* mutants. Comparison of *mud2*-Δ and *msl5* conditional mutants generated in an isogenic background revealed that *mud2*-Δ showed only subtle splicing defects (consistent with previous results, Rain and Legrain, 1997) that were always weaker than in the *msl5* mutants (Figure 40). More importantly, in these strains the leakage of pre-mRNA was increased only about five-fold by a *MUD2* deletion, compared to 20- to 40-fold for the *msl5*

mutants (Figure 40 and Figure 37, see also Rain and Legrain, 1997). This suggests that quantitative effects on splicing and pre-mRNA leakage could be responsible for the difference in the requirement for the functions of *MUD2* and *MSL5*.

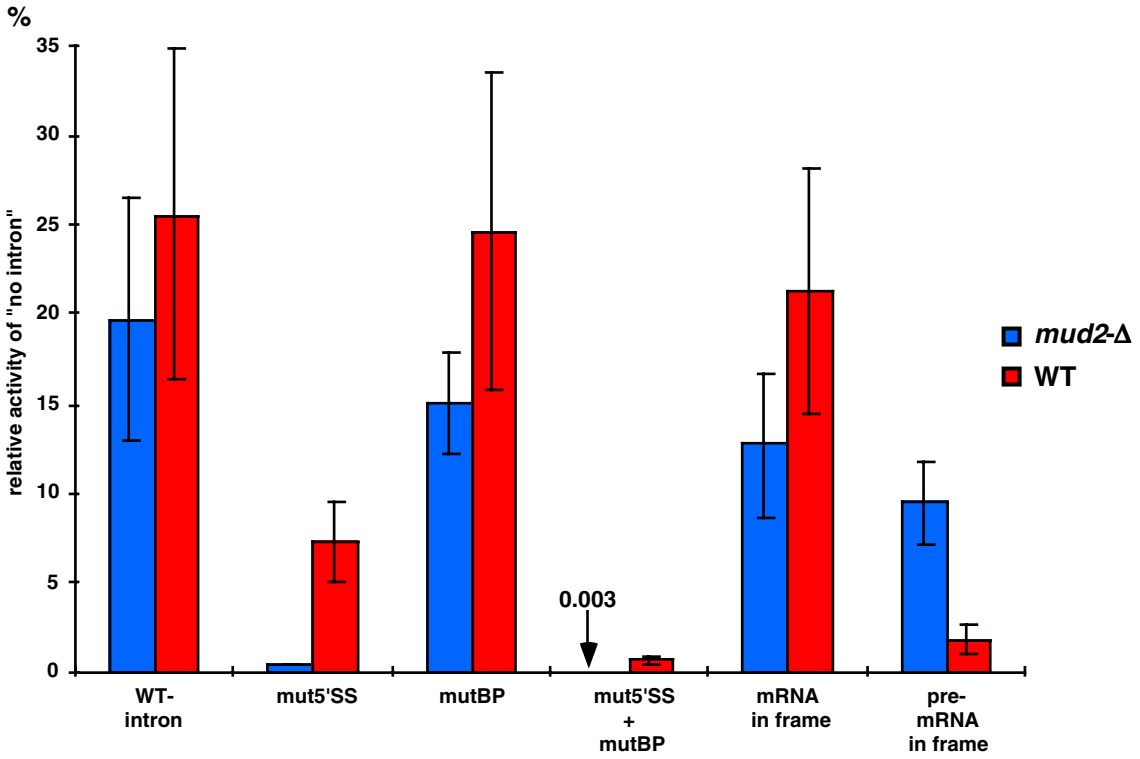

Figure 40. Splicing and pre-mRNA leakage in *mud2*-Δ strain

The reporters contained the RP51A intron in the wild type form (WT-intron) or with a mutation in the 5' splice site (mut5'SS), in the branchpoint (mutBP) or in both (mut5'SS+mutBP) interrupting the reading frame of the *lacZ* gene. Another set of reporters contained a synthetic intron, which was designed in a way that either the mRNA (mRNA in frame) or the pre-mRNA (pre-mRNA in frame) would code for β-galactosidase. Activity is expressed as the relative activity of a construct containing no intron in the *lacZ* gene.

2.7. Temperature-sensitive mutants of *msl5* show a synthetic phenotype with a mutation in the nonsense-mediated decay pathway

Our observation that conditional mutations in *MSL5* result in significant pre-mRNA leakage to the cytoplasm suggested that (part of) the essential function of this protein may reside in its ability to prevent escape of unspliced pre-mRNA from the nucleus. Large amounts of cytoplasmic pre-mRNA could lead to the production of truncated polypeptides that could be directly or indirectly toxic to the cell. Since it has been shown that cytoplasmic pre-mRNA that contains in frame stop codons in the intron is detected and degraded by the NMD pathway (reviewed in Hilleren and Parker, 1999; Czaplinski *et al.*, 1999), we analyzed whether conditional *msl5* mutants would have a synthetic phenotype with

mutants implicated in the NMD pathway in yeast. While this pathway is not essential in yeast, we reasoned that mutations in this pathway could become deleterious if pre-mRNA leakage was abnormally high and toxic for the cell. Therefore, we generated haploid strains carrying either of the three ts mutants that we had analyzed *in vivo* (*msl5-2*,-3,-9) together with a disruption of *upf1*, a helicase involved in the NMD pathway (Leeds *et al*., 1991). These strains were then further analyzed for their growth properties at different temperatures to assay for possible synthetic phenotypes. A difference between strains containing the *UPF1* gene and those disrupted for *UPF1* became obvious at higher temperatures (Figure 41). At 30°C, the *msl5-2* mutant did not grow and the *msl5-3* and -9 mutants were strongly reduced in growth when *UPF1* was disrupted even though the same *msl5* mutants were still able to grow in a *UPF1* background. At 33°C, *msl5-3* did not grow and *msl5-9* grew much more slowly when *UPF1* was disrupted. At 37°C, *msl5-2* and -3 did not grow, while *msl5-9* showed very slow growth when *UPF1* was present and no growth in the context of a *UPF1* disruption. Importantly, deletion of the *UPF1* gene in a wild type *MSL5* background did not affect growth at any temperature (Figure 41). It is noteworthy that the requirement for *UPF1* correlates well with the severity of the leakage in the mutants: the *msl5-2* mutant which has the strongest growth phenotype is synthetic lethal with *upf1*-D already at 30°C, while *msl5-9*, which has a more modest growth phenotype and also shows less pre-mRNA leakage, is synthetic lethal only at 37°C.

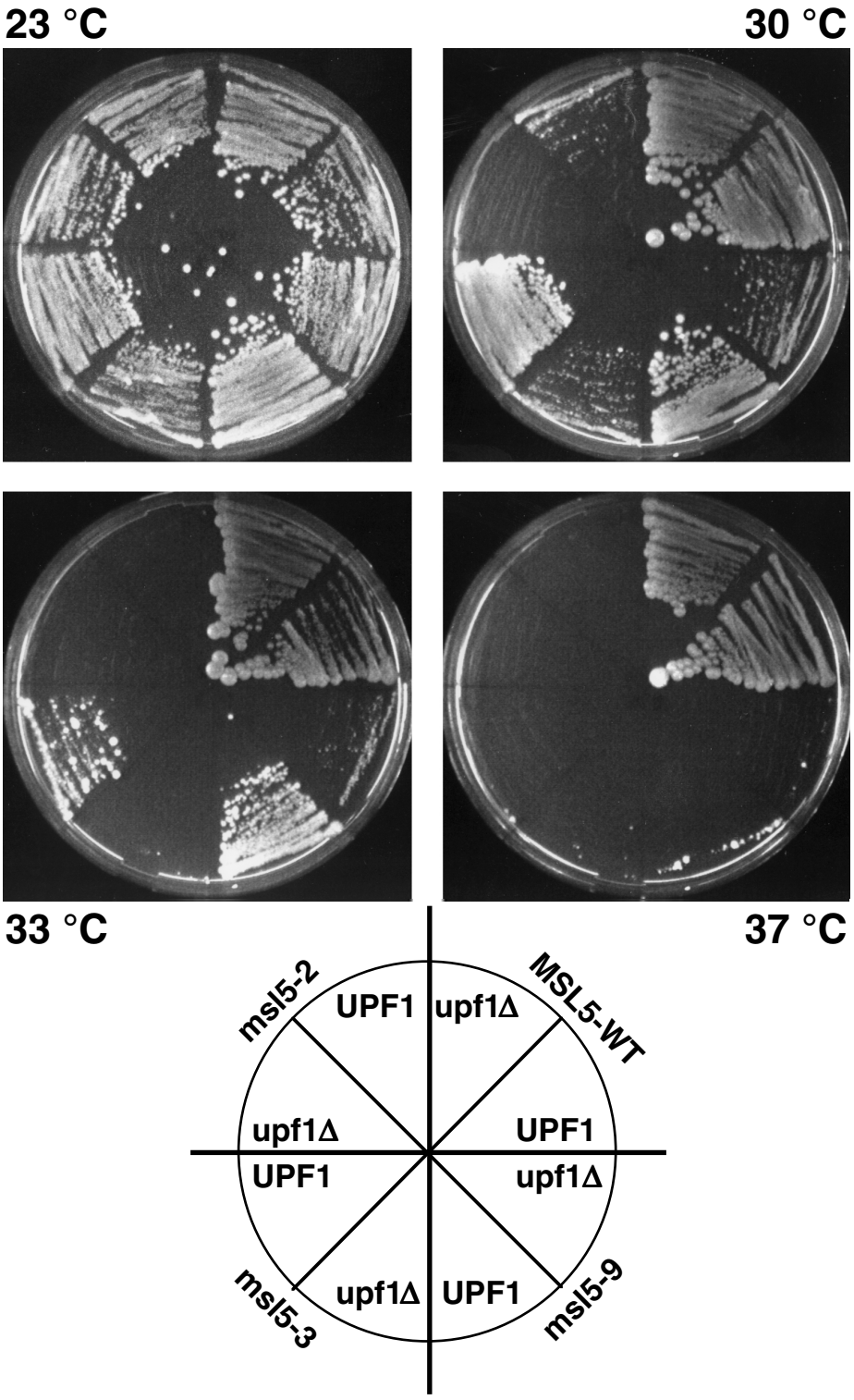

Figure 41. Synthetic lethality of *msl5*-mutants with *upf1*-Δ

Strains containing *msl5-2*, *-3*, *-9* mutants or a wild type copy of *MSL5* (*MSL5*-WT) were compared for their growth at different temperatures with isogenic strains carrying in addition a disruption of the *UPF1* gene (*upf1*Δ). The orientation of the different strains is indicated in a cartoon below the images.

Furthermore, synthetic growth phenotypes were not detected in strains carrying a *UPF1* disruption combined with a deletion of either *NAM8*, *LEA1* or *MUD2* (Figure 42). As *NAM8*, *LEA1* or *MUD2* deletions generate splicing phenotypes similar to the one observed in *msl5* mutants (Rain and Legrain, 1997; Caspary and Séraphin, 1998; Puig *et al*., 1998) but no or only limited pre-mRNA leakage to the cytoplasm (Figure 40; Rain and Legrain, 1997; O. Puig, F. Caspary, personal communication), we conclude that the synthetic phenotype in the *upf1*-Δ background is specifically related to the strong increase in pre-mRNA leakage rather than to the splicing defect of the *msl5* mutants.

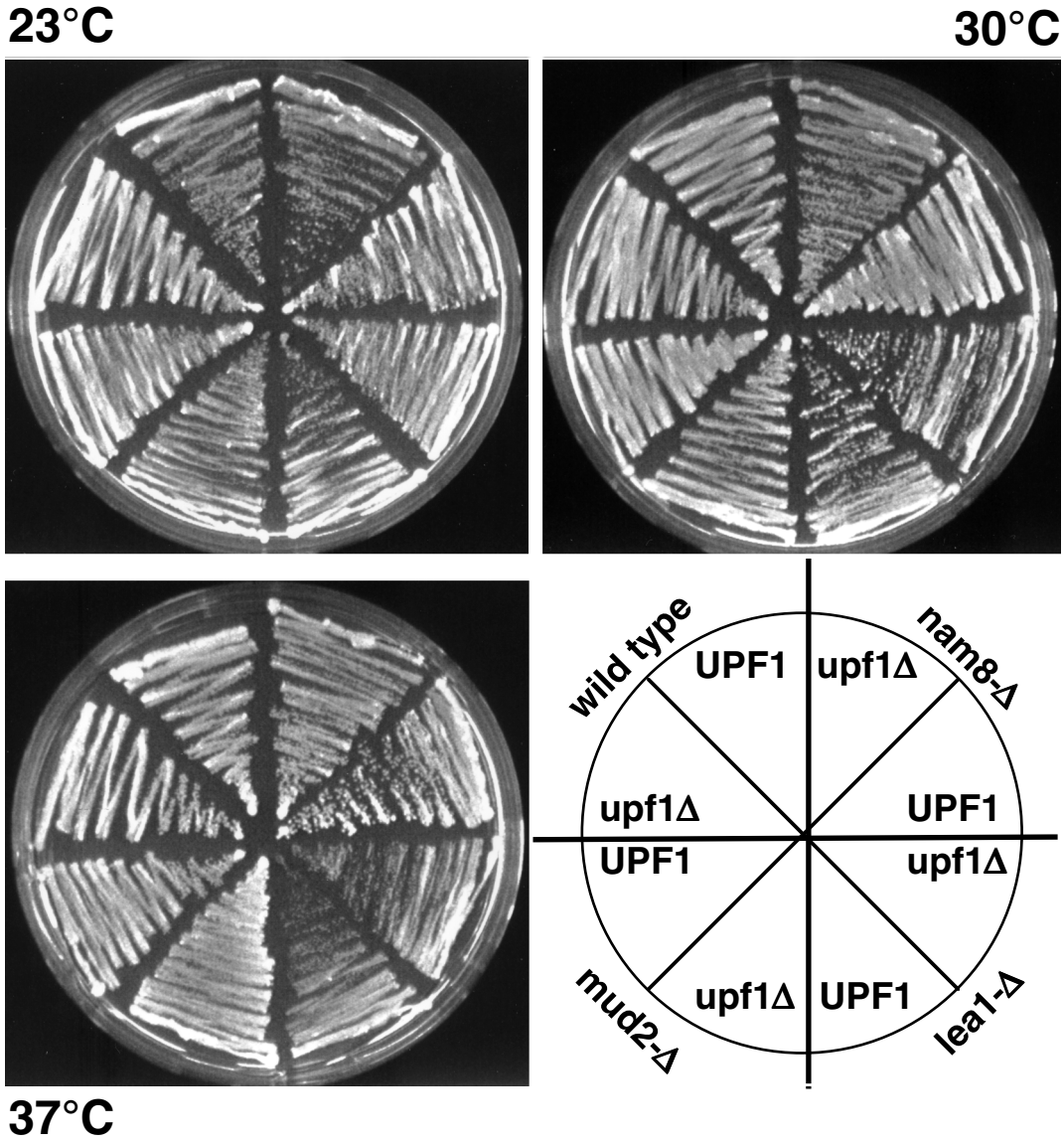

Figure 42. Disruption of *Mud2*, *Lea1* and *Nam8* in combination with *upf1*-Δ

The double disrupted strains were streaked side by side with the corresponding single disrupted strains and were assayed for growth at three different temperatures. Note that all strains are isogenic apart from the genomic disruptions. The position of the different strains is indicated in the cartoon in the lower right corner.

These results demonstrate that the NMD pathway becomes critical when BBP/ScSF1 function is altered. Our results therefore indicate a tight interplay of splicing, pre-mRNA retention and NMD. Given the strong pre-mRNA leakage phenotype of conditional *msl5* mutants, this further suggests that accumulation of unspliced pre-mRNA in the cytoplasm is toxic for the cell. This supports the idea that a function of BBP/ScSF1 is to prevent the negative consequences of pre-mRNA leakage to the cytoplasm.